Catal Lett (2012) 142:1043–1048
DOI 10.1007/s10562-012-0883-4

PERSPECTIVE

Opportunities for Tailoring Catalytic Properties Through Metal-Support Interactions

M. Cargnello · P. Fornasiero · R. J. Gorte

Received: 16 July 2012 / Accepted: 21 July 2012 / Published online: 7 August 2012

Abstract The oxides used as supports for metal catalysts can be used to modify the catalyst properties. In this paper, we discuss three relatively new ways for optimizing the oxide–metal interactions and show examples where these methods have been used to improve catalytic performance. Opportunities still exist for using each of these approaches to produce materials with improved catalytic performance.

Keywords Heterogeneous catalysis · Nanostructure · Colloidal synthesis

1 Introduction

Interactions between metal catalysts and oxide supports have been known to be important for many years. Although oxide supports are primarily used with metal catalysts to maintain metal dispersion, some early work by Schwab and coworkers [1] reported large changes for metal catalysts supported on semiconducting oxides and suggested that electron transfer between the oxide and the metal phases, similar to what occurs in Schottky barriers, was responsible for modifying the properties of the metal. Because electron densities in metals are so much larger than electron densities in semiconducting oxides, such long-range electron transfer is no longer believed to be important, at least for particles larger than about 2 nm; however, there clearly are a number of ways that contact between an oxide and a metal can influence rates and selectivities for reactions, dramatically in some cases. Therefore, understanding and controlling oxide–metal interactions provides an opportunity for improved catalytic performance.

For reducible oxides, such as ceria, the role of the support is at least partially to transfer oxygen to or from the metal. Evidence for this has been presented for ceria-supported metals in the water–gas-shift (WGS) [2], methane-steam-reforming [3], and CO_2-reforming [4] reactions. Reduced ceria has been shown to be oxidized by steam or CO_2 [4], with the oxidized ceria then being reduced by transfer of its oxygen to the metal [5]. Oxygen transfer appears to be important as well for methane combustion over Pd on ceria and other reducible supports [6, 7]. The most active phase for methane oxidation is PdO; however, PdO transforms to metallic Pd at temperatures between 650 and 850 °C. It has been reported that PdO can be stabilized in catalysts containing the rare earths La_2O_3, Pr_2O_3, and CeO_2, with Pr_2O_3-promoted catalysts stabilizing PdO to 1,300 °C [8, 9]. Because these reactions require contact between the oxide and the metal, catalytic performance should be optimized by increasing the interfacial contact between the two phases.

An oxide can also form bonding interactions with a metal catalyst that can in turn modify the adsorption/reaction properties of a metal. One clear case for bonding interactions between a metal and an oxide occurs with titania-supported metals that have been reduced at high temperatures. A manifestation of this bonding interaction is that reduced titania can migrate onto metal particles [10]

M. Cargnello
Department of Chemistry, University of Pennsylvania,
Philadelphia, PA 19104, USA

P. Fornasiero
Department of Chemical and Pharmaceutical Sciences, ICCOM-CNR, Consortium INSTM, University of Trieste, 34127 Trieste,
Italy

R. J. Gorte (✉)
Department of Chemical and Biomolecular Engineering,
University of Pennsylvania, Philadelphia, PA 19104, USA
e-mail: gorte@seas.upenn.edu

and then spread over the metal surface [11]. Because reduced support species migrate onto the metal, separating the effects of TiO_x overlayers from the underlying bonding interactions is probably not possible. In less extreme cases, bonding interactions between a metal and its support simply modify the interfacial energy between the oxide and the metal. Surface energies, associated with both the metal–vacuum and metal–oxide interfaces [12], have been shown to be significant in changing the thermodynamic equilibrium properties of supported Co catalysts to such an extent that CoO can be formed under the relatively reducing conditions of the Fischer–Tropsch Synthesis reaction, even though metallic Co is the predicted phase [13, 14]. As in the case with reducible oxides that transfer oxygen, supported metal catalysts that are affected by bonding interactions must have direct contact between the phases, so that any potential advantages associated with these effects would require maximizing the interface between the oxide and the metal.

With alkali promoters, it has been shown that through-space electric fields can influence metal sites over a relatively long distance [15]. Some evidence that these kinds of effects may be important in supported-metal catalysis comes from a recent study that showed greatly enhanced rates for the WGS reaction over Pt/alumina catalysts when alkalis were doped into the alumina [16]. Again, if field effects are important, the sites on the metal catalyst that would be modified could not extend more than ~1 nm from the oxide–metal interface, since this is the distance over which alkali promoters are typically important. In some cases, it is still uncertain how oxide supports modify a metal catalyst. Indeed, it is likely that a combination of the above factors is responsible for the novel properties of Au/titania catalysts. Still, there is strong evidence that the most active sites are those at the interface between Au and titania [17, 18].

The above discussion demonstrates that maximizing oxide–metal interactions requires maximizing the concentration of interfacial sites. While this can be done in normal catalysts by increasing the dispersion of a metal catalyst on a support oxide, a number of other approaches for achieving maximal contact have appeared in the literature in recent years. We believe this represents an important opportunity for preparing and modifying catalysts to improve their properties and therefore wish to highlight some of these approaches.

2 Ex-solution Catalysts

Loss of metal surface area through sintering is a serious problem in automotive catalysis and engineering the oxide–metal interactions to minimize this and other problems that occur in these catalysts is practiced at an extremely sophisticated level. One of the most interesting concepts to come out of this area is that of using "ex-solution" to maintain metal dispersion. The basic idea is that metal ions, like Pd^{2+}, can reversibly enter some oxide lattices, notably those with the relatively open perovskite structure, such as $LaFeO_3$ or $BaCeO_3$ [19, 20]. When exposed to reducing conditions, the noble-metal ions are released by the oxide host in the form of catalytically-active, metal nanoparticles. This ex-solution process is shown schematically in Fig. 1. The use of this approach is reported to greatly enhance the thermal stability of three-way automotive exhaust catalysts, to an extent that the precious metal does not coarsen even after extended periods at high temperatures (up to 1,000 °C). It has been reported that this strategy makes it possible to reduce the amount of precious metal that is required in automotive catalysts compared to that in conventional catalytic converters.

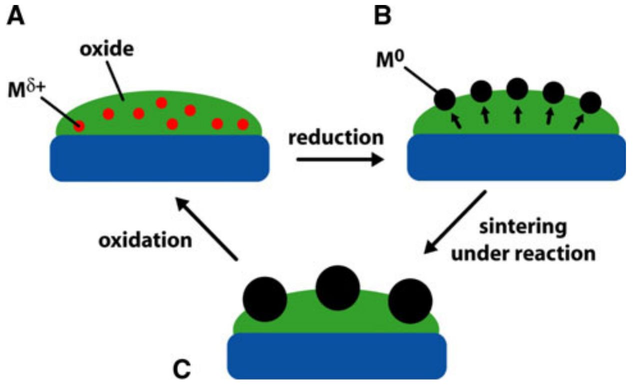

Fig. 1 Schematic representation of the "ex-solution" process. **a** Metal ions in high oxidation states can enter the oxide lattice. **b** Reducing conditions cause the release of the metal ions in form of metallic particles on the surface of the oxide. **c** Sintering under reaction conditions increases the metal particle size, but oxidation is capable of bringing the system back to its initial state (**a**)

Ex-solution concepts have also been used in solid oxide fuel cells (SOFC) to incorporate catalytic components into ceramic conductors for anode applications [21–23]. The first instance of using this approach that we are aware of involved incorporating Ru into Sr-doped $LaCrO_3$ [24]. Under the reducing conditions experienced by the SOFC anode during operation, metallic Ru forms at the oxide surface, providing catalytic activity that significantly improves the electrode performance. More recently, Ni, Co, and Cu ions have been incorporated into the $LaVO_4$ and $CeVO_4$ lattices, then removed by ex-solution as metal particles upon reduction [23]. However, other than using ex-solution concepts for maintaining metal dispersion in three-way automotive catalysts and SOFC anodes, the properties of these catalysts have not been extensively investigated.

There are indications that materials prepared by ex-solution could have unique catalytic properties. A study of methane-steam-reforming rates on $La_{0.8}Sr_{0.2}Cr_{0.98}Ru_{0.02}O_3$ showed that this catalyst maintained high activities at a H_2O:C ratio of 0.1 without coking [25]. Although the authors of this study suggested that the active phase in their catalyst was Ru(IV) in the perovskite lattice, it is more likely that the properties observed in the steam-reforming study were those of small Ru particles or clusters formed by ex-solution, in close contact with the perovskite support. First, Ru nanoparticles were formed from a very similar material and under similar conditions in the SOFC anode work [21, 22]. Furthermore, the steam-reforming environment is sufficiently reducing that metallic Ru is the expected phase. The suppression of coke formation in this ex-solution catalyst is likely caused by having the support maintain very small metal particles or through strong interactions between the metal particles and the underlying perovskite. That the perovskite support could have such a large impact on the metallic Ru particles is intriguing.

It is also possible that metal cations could be stabilized by the oxide environment, as the authors suggested. Considering the somewhat simpler case of Ni, equilibrium considerations imply that there is a well-defined $P(O_2)$ associated with the oxidation reaction, as shown in Eq. (1).

$$\begin{aligned} &Ni + \tfrac{1}{2}O_2 \rightleftharpoons NiO \\ &K_{Ni} = P(O_2)^{-1/2} = \exp\{-\Delta G_{Ni}/RT\} \end{aligned} \quad (1)$$

At $P(O_2)$ higher than that defined by Eq. (1), only NiO will be present at equilibrium; at $P(O_2)$ lower than this, only metallic Ni will be formed. Although there is no gas-phase oxygen present under steam-reforming conditions, there is an equivalent $P(O_2)$ associated with the chemical potential established by equilibrium between H_2 and H_2O or CO and CO_2 [26]. If NiO in Eq. (1) is replaced by La_2NiO_4, as in Eq. (2), ΔG and the equilibrium $P(O_2)$ for the reaction of Ni to Ni^{2+} could change.

$$\begin{aligned} &La_2O_3 + Ni + \tfrac{1}{2}O_2 \rightleftharpoons La_2NiO_4 \\ &K_{LNO} = P(O_2)^{-1/2} = \exp\{-\Delta G_{LNO}/RT\} \end{aligned} \quad (2)$$

That the effect of having a mixed oxide could be dramatic is demonstrated by comparing the V^{3+}–V^{5+} redox couple in $LaVO_4$ and $CrVO_4$. In this case, the equilibrium $P(O_2)$ is lower by a factor of 10^{16} in $LaVO_4$ at 973 K [27]. Therefore, it is certainly possible that the presence of the mixed oxide could enhance catalytic properties by stabilizing metal cations in an oxide lattice.

Whatever mechanisms are responsible for changes in the catalytic properties of metals that are initially part of a perovskite or other mixed oxide lattice, it is apparent that these catalysts represent a relatively untapped opportunity to tune reaction properties for beneficial effects, particularly for high-temperature applications. Because the perovskite structure is common and is formed from a large number of mixed oxides, results will likely be different, not only for the various metal catalysts, but also for different perovskite hosts, so that ex-solution materials could represent an entirely new area for research.

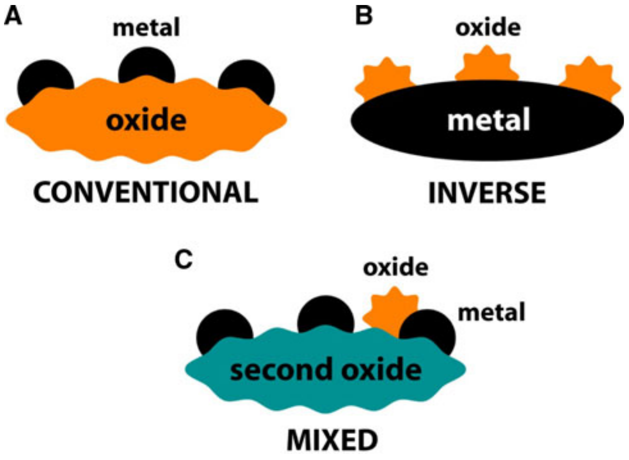

Fig. 2 Schematic representation of a conventional catalyst (**a**), where a metal is deposited onto an oxide support; an inverse catalyst (**b**), where the oxide is deposited onto a metallic support; and a mixed system (**c**), where both the metal and the promoter oxide are co-deposited onto a second oxide support

3 Inverse Catalysts

Because many of the oxide–metal interactions that affect catalytic properties are associated with the interface between the two phases, some have proposed that these interactions be achieved by preparing “inverse catalysts” [28], where the oxide is incorporated onto the metal, rather than the conventional case of having the metal on the oxide. The idea is shown schematically in Fig. 2. The concept of incorporating oxides onto bulk metals to make model catalysts for mechanistic studies is certainly not new. Model catalysts based on titania overlayers on bulk, group VIII metals played an important role in figuring out the causes behind what had been known as strong metal-support interactions (SMSI) [11, 29]. These “flat” catalysts are much easier to characterize by standard surface-science techniques, like X-ray photoelectron spectroscopy (XPS) and temperature programmed desorption.

What is new is the idea of using this concept in real, high-surface-area catalysts. Here, the “support” oxide is used as a promoter for the catalyst. In principle, the catalyst could be supported on a second oxide, as demonstrated by the “Mixed” configuration in Fig. 2. Again, the use of catalyst promoters is not new; but the fabrication of catalysts with novel structures and the use of support-oxides as promoters is novel. Since a Perspectives article has already been published on this subject [30], we simply provide two examples for illustration.

The first example is that of a CuO–CeO_2 catalyst for the selective oxidation of CO in the presence of H_2 (PROX) [31]. The authors prepared their inverse catalysts using a microemulsion method that, in the as-synthesized form, consisted of larger CuO crystals, decorated by smaller CeO_2 crystallites. In this case, the active phase was CuO, rather than metallic Cu because reduction to metallic Cu resulted in a loss of selectivity due to increased activity for H_2 oxidation. Interactions between the CuO and CeO_2 appear to be critical for maintaining the Cu in its oxidized form. In situ XRD measurements demonstrated that reduction of CuO to Cu occurred over a very narrow temperature range, near 470 K, with ceria simultaneously undergoing significant reduction in exactly the same temperature region. Interestingly, the authors reported that a $Cu_{0.2}Ce_{0.8}O_2$ sample became reduced at a lower temperature and was therefore nonselective.

The second example involves catalysts for the oxidative dehydrogenation (ODH) of ethane to ethylene over a conventional Pd/Al_2O_3 catalyst that was modified by depositing Al_2O_3 overlayers using Atomic Layer Deposition (ALD) [32]. In ALD, oxide monolayers are deposited onto a conventional Pd/Al_2O_3 catalyst by first reacting the surface with an organometallic compound (trimethylaluminum in this case), then oxidizing that surface (e.g. by exposure to water vapor). The advantage of this approach is that a very uniform, oxide film is formed over the entire surface of the catalyst. In this ODH study, the authors reported that the conventional Pd/Al_2O_3 catalyst coked up rapidly under reaction conditions, while the modified catalyst was active and completely stable, with minimal coke production and excellent selectivity towards ethylene. Based on FTIR measurements of adsorbed CO, the authors inferred that the Al_2O_3 overlayers blocked low-coordination sites on the Pd crystallites that were believed to be involved in coke formation and metal sintering. For this example, then, no chemical interaction was required for the oxide overlayer to modify the properties of the metal, so that the modifications demonstrated a way to tailor the physical properties of the catalyst through the manipulation of the metal-support morphology.

4 Core–Shell Catalysts

Another way of maximizing oxide–metal interactions and preventing the coalescence of the metal nanoparticles into larger particles at medium-to-high reaction temperatures involves producing metal@oxide, core–shell catalysts. Core–shell concepts have been pursued most heavily for bimetallic systems, especially with applications in fuel-cell electrodes, where the metal core effectively modifies the electronic properties of the surface atoms in the metal shell [33]. There have been fewer (but growing in number) studies focusing on catalysts in which the shell is an oxide. Although some have suggested that the presence of a group VIII metal [34] or metal cations [35] within the oxide may modify the properties of the catalytic oxide, for most applications one should probably view the oxide shell as being porous, so that reactant molecules can access sites on the metal core.

The preparation of core–shell catalysts has been accomplished using one of four general procedures, or some combination of these, shown schematically in Fig. 3. Although each procedure generally starts with preformed metal particles (or their precursors) which are then coated with the metal–oxide, the detailed structures that are obtained differ rather dramatically depending on how the synthesis is carried out. The first procedure shown in Fig. 3 is used to make egg-yolk structures, in which the metal core is in a void volume made from a larger oxide shell [36]. The synthesis takes advantage of properties that are specific to silica, directly coating the metal particles with the silica layer through the slow and controllable hydrolysis of silicon alkoxides. To produce the egg-yolk structure, a second oxide is grown on top of the silica, after which the silica is dissolved away. This type of core–shell particle is of interest for isolating metal crystallites but clearly does not maximize oxide–metal interfacial contact.

In the second procedure in Fig. 3, the preformed metal particles (or their precursors) are precipitated together with the metal–oxide precursor (co-precipitation). This method is relatively simple to carry out but does not generally provide great control over the final catalyst structure. Somewhat better control is achieved using microemulsions as a nanoreactor, the third procedure in Fig. 3. Here, the metal particles are produced inside micelles, which are in turn coated with the metal–oxide precursor to form the encapsulated metal.

Our groups have recently used self-assembly methods to achieve even better control, allow a finer tuning of the oxide shell, and better maximize the metal–oxide interactions [37–39]. The first step in the synthesis of the core–shell structures involves synthesizing metal nanoparticles that are maintained in non-polar solutions using thiol ligands. The thiols are chosen to have carboxyl end groups that can be used to react with metal alkoxides. Following a controlled, partial hydrolysis in the presence of a long-chain organic acid, an M@oxide particle is produced that is soluble in low-polarity solutions. The method produces highly uniform particles, with metal particles approximately 2 nm in diameter and oxide shells on the order of 2 nm thick. The method is flexible and has been used to

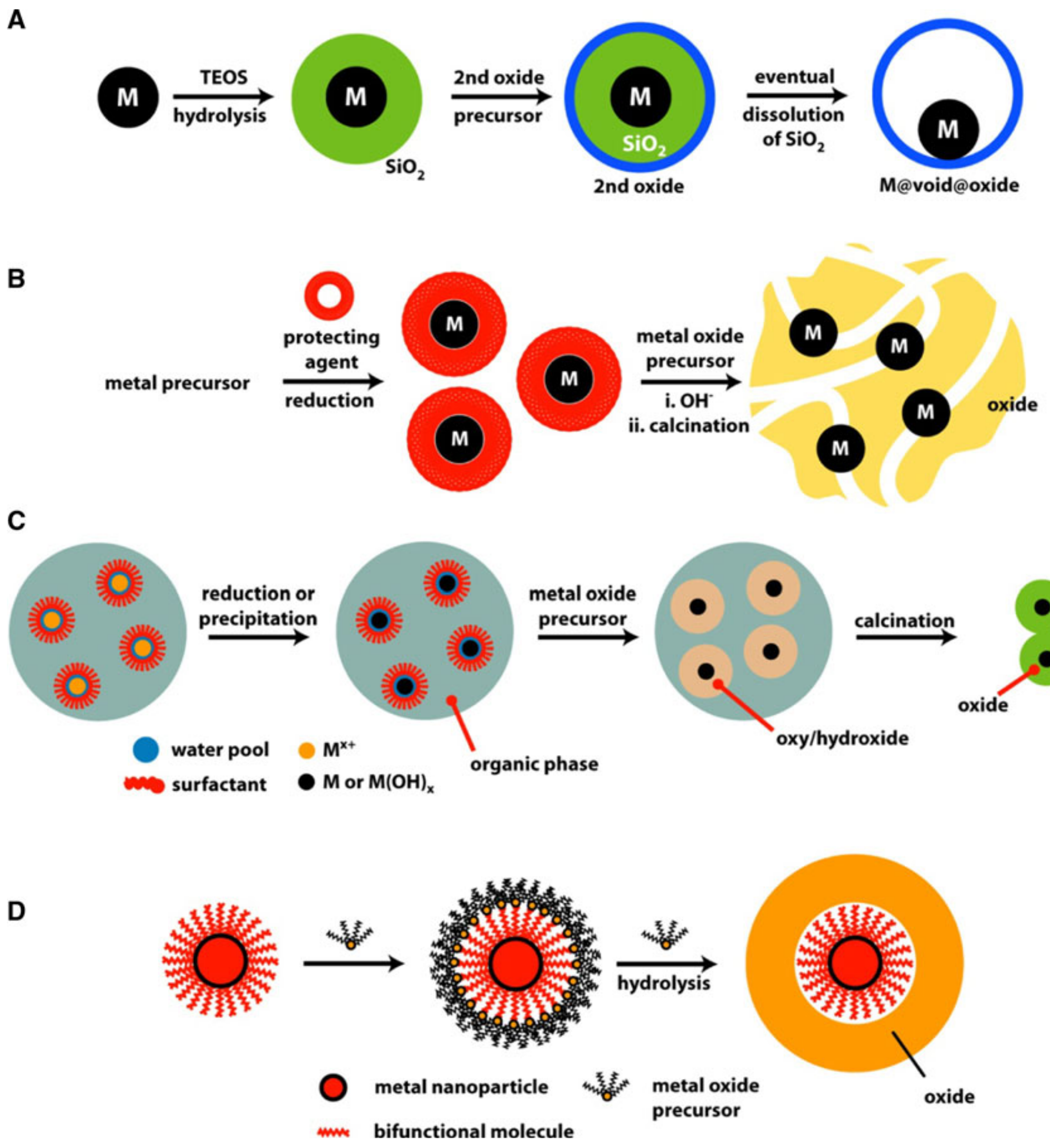

Fig. 3 Schematic representation of synthetic strategies for the preparation of core–shell type catalysts. **a** Silica coating of metal particles and eventual formation of a second oxide coating and dissolution of silica. **b** Co-precipitation of preformed metal particles and metal–oxide precursor. **c** Microemulsion-mediated synthesis. **d** Functionalization of a metal particle surface and subsequent reaction with the metal- oxide precursor to build the oxide shell around the metal core

produce Pd and Pt nanoparticles with shells of ceria, zirconia, and titania [37]. Because these core–shell particles are dispersed in non-aqueous solutions, they can be adsorbed onto functionalized supports to achieve a monolayer of M@oxide particles on a second oxide.

We have only begun to explore the catalytic properties of these core–shell structures but the initial results are very exciting. In an application involving anodes in solid oxide fuel cells, Pd@ceria core–shell catalysts were found to exhibit excellent catalytic performance and much improved stability against metal sintering at high temperatures compared to a conventional Pd/ceria catalyst [40]. Even more exciting, Pd@ceria core–shell structures that were deposited as single entities onto a modified, hydrophobic alumina support exhibited exceptional activity for methane combustion, with rates more than a factor of 10 higher than the best Pd/ceria catalyst we could make, and showed stable activity to at least 850 °C [41]. In this application, it appears that the very close proximity between Pd and ceria prevented Pd sintering and stabilized Pd as PdO.

5 Conclusions

Opportunities exist for using oxide–metal interactions to achieve improved catalytic properties. Three relatively new approaches for maximizing these interactions are described here: (1) Ex-Solution of metals from mixed oxides; (2) Inverse catalysts in which the oxide is placed over the metal, and (3) Core–shell catalysts with oxide shells over the metal core. We believe that these three approaches provide important opportunities for future developments in heterogeneous catalysis.

Acknowledgments RJG acknowledge support for this work from the Department of Energy, Office of Basic Energy Sciences, Chemical Sciences, Geosciences and Biosciences Division, Grant DE-FG02-85ER13350. MC and PF acknowledge financial support from University of Trieste through FRA 2011 project.

References

1. Schwab G-M, Koller K (1968) J Am Chem Soc 90:3078
2. Bunluesin T, Gorte RJ, Graham GW (1998) Appl Catal B 15:107
3. Craciun R, Shereck B, Gorte RJ (1998) Catal Lett 51:149
4. Sharma S, Hilaire S, Vohs JM, Gorte RJ, Jen H-W (2000) J Catal 190:199
5. Smirnov MY, Graham GW (2001) Catal Lett 72:39
6. Schwartz WR, Pfefferle LD (2012) J Phys Chem C 116:8571
7. Schwartz WR, Ciuparu D, Pfefferle LD (2012) J Phys Chem C 116:8587
8. Farrauto RJ, Hobson MC, Kennelly T, Waterman EM (1992) Appl Catal A81:227
9. Farrauto R, Lampert J, Hobson M, Waterman E (1995) Appl Catal B 6:263
10. Sadeghi HR, Henrich VE (1984) J Catal 87:279
11. Ko CS, Gorte RJ (1984) J Catal 90:59
12. van Steen E, Claeys M, Dry ME, van de Loosdrecht J, Viljoen EL, Visagie JL (2005) J Phys Chem B 109:3575–3577
13. Bezemer GL, Bitter JH, Kuipers HPCE, Oosterbeek H, Holewijn JE, Xu X, Kapteijn F, van Dillen AJ, de Jong KP (2006) J Am Chem Soc 128:3956–3964
14. Bakhmutsky K, Wieder NL, Baldassare T, Smith MA, Gorte RJ (2011) Appl Catal A 397:266–271
15. Uram KJ, Ng L, Yates JT (1986) Surf Sci 177:253
16. Zhai YP, Pierre D, Si R, Deng WL, Ferrin P, Nilekar AU, Peng GW, Herron JA, Bell DC, Saltsburg H, Mavrikakis M, Flytzani-Stephanopoulos M (2010) Science 329:5999
17. Shekhar M, Wang J, Lee WS, Williams WD, Kim SM, Stach EA, Miller JT, Delgass WN, Ribeiro FH (2012) J Am Chem Soc 134:4700–4708
18. Green IX, Tang W, Neurock M, Yates JT (2011) Science 333:736–739
19. Nishihata Y, Mizuki J, Akao T, Tanaka H, Uenishi M, Kimura M, Okamoto T, Hamada N (2002) Nature 418:164–167
20. Li J, Singh UG, Bennett JW, Page K, Weaver JC, Zhang J-P, Proffen T, Rappe AM, Scott S, Seshadri R (2007) Chem Matls 19:1418
21. Kobsiriphat W, Madsen BD, Wang Y, Marks LD, Barnett SA (2009) Solid State Ionics 180:257–264
22. Bierschenk DM, Potter-Nelson E, Hoel C, Liao YG, Marks L, Poeppelmeier KR, Barnett SA (2011) J Power Sources 196:3089–3094
23. Adijanto L, Balaji Padmanabhan V, Küngas R, Gorte RJ, Vohs JM (2012) J Mater Chem 22:11396–11402
24. Wang Y, Madsen BD, Kobsiriphat W, Barnett SA, Marks LD (2007) Microsc Microanal 13:100
25. Caillot T, Gauthier G, Delichere P, Cayron C, Cadete FJ, Aires S (2012) J Catalysis 290:158
26. Shah PR, Kim T, Zhou G, Fornasiero P, Gorte RJ (2006) Chem Mater 18:5363
27. Shah PR, Khader MM, Vohs JM, Gorte RJ (2008) J Phys Chem C 112:2613
28. Rodriguez JA, Ma S, Liu P, Hrbek J, Evans J, Pérez M (2007) Science 318:1757–1760
29. Williams KJ, Salmeron M, Bell AT, Somorjai GA (1988) Surf Sci 204:L745
30. Rodriguez JA, Hrbek J (2010) Surf Sci 604:241
31. Hornés A, Hungría AB, Bera P, Lopéz Cámara A, Fernández-García M, Martínez-Arias A, Barrio L, Estrella M, Zhou G, Fonseca JJ, Hanson JC, Rodriguez JA (2010) J Am Chem Soc 132:34–35
32. Lu J, Fu B, Kung MC, Xiao G, Elam JW, Kung HH, Stair PC (2012) Science 335:1205–1208
33. Greeley J, Norskov JK, Kibler LA, El-Aziz AM, Kolb DM (2006) Chem Eur J Chem Phys 7:1032–1035
34. Yeung CMY, Yu KMK, Fu QJ, Thompsett D, Petch MI, Tsang SC (2005) J Am Chem Soc 127:18010–18011
35. Fu Q, Saltsburg H, Flytzani-Stephanopoulos M (2003) Science 301:935–938
36. Guttel R, Paul M, Galeano C, Schuth F (2012) J Catalysis 289:100
37. Bakhmutsky K, Wieder NL, Cargnello M, Galloway B, Fornasiero P, Gorte RJ (2012) Chem Sus Chem 5:140–148
38. Cargnello M, Wieder NL, Montini T, Gorte RJ, Fornasiero P (2010) J Am Chem Soc 132:1402–1409
39. Cargnello M, Wieder NL, Canton P, Montini T, Giambastiani G, Benedetti A, Gorte RJ, Fornasiero P (2011) Chem Mater 23:3961–3969
40. Kim JS, Wieder NL, Abraham AJ, Cargnello M, Fornasiero P, Gorte RJ, Vohs JM (2011) J Electrochem Soc 158:B596–B600
41. M. Cargnello, J. J. Delgado Jaén, J. C. Hernández Garrido, K. Bakhmutsky, T. Montini, J. J. Calvino Gamez, R. J. Gorte, P Fornasiero (2012) Science. doi:10.1126/science.1222887